

Design Principles and Routes for Calcium Alkoxyaluminate Electrolytes

Noel J. Leon, Stefan Ilic, Xiaowei Xie, Heonjae Jeong, Zhenzhen Yang, Bingning Wang, Evan Walter Clark Spotte-Smith, Charlotte Stern, Nathan Hahn, Kevin Zavadil, Lei Cheng, Kristin A. Persson, Justin G. Connell, and Chen Liao*



Cite This: *J. Phys. Chem. Lett.* 2024, 15, 5096–5102



Read Online

ACCESS |



Metrics & More

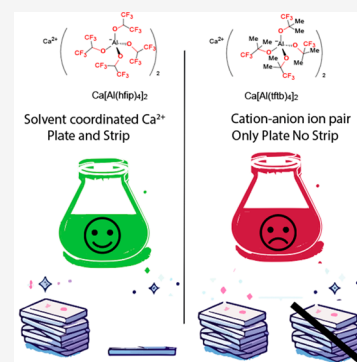


Article Recommendations



Supporting Information

ABSTRACT: Multivalent-ion battery technologies are increasingly attractive options for meeting diverse energy storage needs. Calcium ion batteries (CIB) are particularly appealing candidates for their earthly abundance, high theoretical volumetric energy density, and relative safety advantages. At present, only a few Ca-ion electrolyte systems are reported to reversibly plate at room temperature: for example, aluminates and borates, including $\text{Ca}[\text{TPFA}]_2$, where $[\text{TPFA}]^- = [\text{Al}(\text{OC}(\text{CF}_3)_3)_4]^-$ and $\text{Ca}[\text{B}(\text{hfp})_4]_2$, $[\text{B}(\text{hfp})_4]_2^- = [\text{B}(\text{OCH}(\text{CF}_3)_2)_4]^-$. Analyzing the structure of these salts reveals a common theme: the prevalent use of a weakly coordinating anion (WCA) consisting of a tetracoordinate aluminum/boron (Al/B) center with fluorinated alkoxides. Leveraging the concept of theory-aided design, we report an innovative, one-pot synthesis of two new calcium-ion electrolyte salts ($\text{Ca}[\text{Al}(\text{tftb})_4]_2$, $\text{Ca}[\text{Al}(\text{hftb})_4]_2$) and two reported salts ($\text{Ca}[\text{Al}(\text{hfp})_4]_2$ and $\text{Ca}[\text{TPFA}]_2$) where $\text{hfp} = (-\text{OCH}(\text{CF}_3)_2)$, $\text{tftb} = (-\text{OC}(\text{CF}_3)(\text{Me})_2)$, $\text{hftb} = (-\text{OC}(\text{CF}_3)_2(\text{Me}))$, $[\text{TPFA}]^- = [\text{Al}(\text{OC}(\text{CF}_3)_3)_4]^-$. We also reveal the dependence of Coulombic efficiency on their inherent propensity for cation–anion coordination.



The increasing prevalence of lithium-ion batteries (LIB) continues to raise concerns over elemental scarcity and the environmental impact of mining crucial resources for cathode and electrolyte materials. Complementary to discovering a direct LIB replacement is the concept of diversifying rechargeable battery chemistries that can be customized for specific applications, such as long-duration energy storage systems and various transportation modes like aviation, rail, and ships.¹ These discussions have fueled the surge in “beyond LIB” research.² Alkaline earth metal-based battery (Mg, Ca) literature offers the advantages of crustal abundance, volumetric density, and overall safety, with a considerably higher focus on Mg electrolyte development.³ The calcium-ion battery (CIB) literature lacks electrolytes that reliably plate and strip calcium metal.^{4–8} CIBs using solid metal anodes (Ca) face additional problems: Ca has a reduction potential only 170 mV higher than that of lithium, which exceeds the thermodynamic stability of most electrolytes, and stabilizing Ca anodes will require a specific interphase that is suitable for continuous stable electrochemical performance. As a result, the design of efficient CIBs is highly dependent on the bulk stability of electrolytes exposed to highly reducing environments during plating and stripping.⁶

Weakly coordinating anions (WCAs) have been used in a variety of chemistries to date and have been found to be highly efficient electrolytes for multivalent (MV) batteries.^{5,9–12} As the name suggests, WCAs leverage the idea of minimizing ion

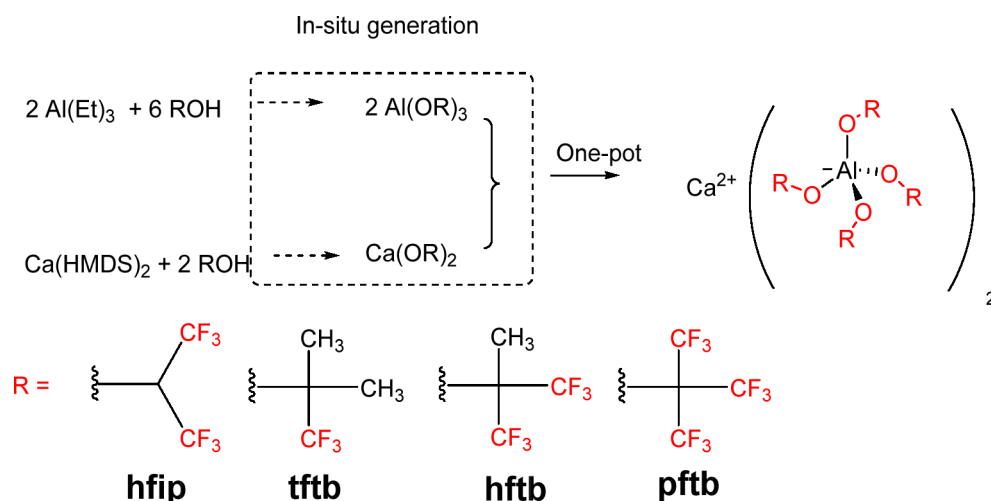
association by utilizing steric bulkiness and uniform charge distribution to stabilize reactive electrophiles, all while remaining chemically innocent. Alkoxyaluminates and alkoxyborates are two groups of WCAs that have found success in recent metal anode investigations due to their excellent reductive and oxidative stability and resulting high Coulombic efficiency.^{5,6,11,13} These alkoxyaluminate and alkoxyborate structures can be designed in multiple ways by substituting alkoxide ligands to target optimal electrolyte characteristics. Two recent computational studies explored the stability of alkoxyaluminate and alkoxyborate salts incorporating a range of alkoxides and their resulting decomposition through density functional theory (DFT) and ab initio molecular dynamics (AIMD) simulations.¹⁴ These data indicate a few target structures that are less likely to decompose.

In this work, we develop a one-pot synthesis giving access to a variety of new calcium alkoxyaluminate analogs. Specifically, the ligands used here are the hexafluoroisopropoxy ($\text{hfp} = -\text{OCH}(\text{CF}_3)_2$), trifluoro-*tert*-butoxy ($\text{tftb} = -\text{OCMe}_2(\text{CF}_3)$), hexafluoro-*tert*-butoxy ($\text{hftb} = -\text{OCMe}(\text{CF}_3)_2$), and perfluoro-

Received: April 2, 2024

Revised: April 19, 2024

Accepted: April 24, 2024

Scheme 1. Successful One-Pot Synthesis Using Ca(HMDS)₂ To Make Calcium WCAs with Alkoxyaluminates

tert-butoxy (pftb = $-\text{OC}(\text{CF}_3)_3$) groups (Scheme 1). Note the aluminate with pftb ligands can also be referred to as tetrakis(perfluoro-*tert*-butoxy)aluminate (TPFA) as in previous publications.^{10,12,15} Using this new one-pot synthetic route, it is both simple and scalable to synthesize two new calcium alkoxyaluminates ($\text{Ca}[\text{Al}(\text{tftb})_4]_2$ and $\text{Ca}[\text{Al}(\text{hftb})_4]_2$) highlighted by previous theoretical work. The other $\text{Ca}[\text{Al}(\text{hfip})_4]_2$ ¹⁶ and $\text{Ca}[\text{Al}(\text{pftb})_4]_2$ ⁷ can also be conveniently synthesized with this improved synthetic method. Contrary to initial assumptions that these electrolytes are all weakly associated, our findings reveal that excessively strong cation–anion ion pair formation is a key factor hindering calcium plating and stripping in the strong Ca^{2+} -anion coordination forming salts of $\text{Ca}[\text{Al}(\text{tftb})_4]_2$. The $\text{Ca}[\text{Al}(\text{hfip})_4]_2$ electrolyte was found to perform considerably better due to its promotion of solvent-coordinated Ca^{2+} .

RESULTS AND DISCUSSION

Previously, a few alkoxyaluminates were identified as reductive stable through computational analysis of the transition states along the decomposition pathways.¹⁴ Among the Ca–Al compounds, a range of ligands were predicted to exhibit higher than 0.6 eV decomposition barriers, and $\text{Ca}[\text{Al}(\text{tftb})_4]_2$ in particular exhibited a 1.0 eV kinetic barrier toward reductive decomposition. To prove such claims, synthetic chemists must rely on intuition and lessons learned through optimization. Two main synthetic routes have prevailed in the synthesis of alkoxyaluminate and borate electrolytes, with challenges associated with each.^{5,6,16} As we describe in the Supporting Information, these methods prove impractical for the desired alkoxyaluminates due to either the presence of unstable bis(diethyloxonium) protonated intermediates^{12,17} or the limited reactivity of the targeted alcohols with calcium methoxide.¹⁸ A new synthetic route is therefore needed to address these problems.

To address these challenges, we report a new synthetic route utilizing a one-pot method with both a soluble calcium base as well as using an intermediate without separations. Previously, $\text{Ca}(\text{OR})_2$ (where OR = hfip) has been synthesized through an exchange reaction between a slurry of $\text{Ca}(\text{OMe})_2$ and hexafluoroisopropanol,¹⁶ however, the less acidic and more sterically bulky tftb and hftb ligands are much less reactive. As shown in Scheme 1, the new route is enabled by a soluble

source of calcium, calcium hexamethyldisilazide ($\text{Ca}(\text{HMDS})_2$). Previous reports use metal hydrides as a source of metal in the acid–base reaction;^{7,15} however, reactions with CaH_2 suffer from similar issues, forming an insoluble slurry, which does not react with ROH. The solution here is to utilize the soluble base of $\text{Ca}(\text{HMDS})_2$. This adaptation effectively bypasses the presence of impurities—the previous TPFA synthesis uses LiAlH_4 and HCl which introduced Li and Cl impurities—while using a relatively simple rearrangement method. $\text{Ca}(\text{HMDS})_2$ is also reactive enough with even less acidic alcohols like tftb. This salt is not commercially available, but it is readily synthesized via a literature method (Section 2 in Supporting Information).

The other innovation here is the one-pot design of reacting $\text{Al}(\text{Et})_3$ with ROH in the presence of $\text{Ca}(\text{OR})_2$, which avoids the separation of the intermediate of $\text{Al}(\text{OR})_3$. The rearrangement of the resulting $\text{Al}(\text{OR})_3$ with $\text{Ca}(\text{OR})_2$ pushes the equilibrium to the right. As shown in Scheme 1, this new rearrangement method via $\text{Ca}(\text{HMDS})_2$ proves to be a reproducible synthetic route to new calcium alkoxyaluminates, including $\text{Ca}[\text{Al}(\text{hfip})_4]_2$ and the previous inaccessible $\text{Ca}[\text{Al}(\text{tftb})_4]_2$. As these two novel materials exhibit distinctive electrochemical stability arising from their distinct solvation environments, the following text will focus on discussing their structural variations and how it significantly impacts electrochemical performance. As shown in the Supporting Information, this route also enables syntheses of calcium alkoxyaluminates with a wide range of ligands including hftb and pftb. The two popular synthetic methods (Schemes S1 and S2 in Supporting Information) proved unsuccessful due to instability of intermediates or the poor solubility, and thus poor reactivity of the calcium source. For example, the attempted synthesis of $[\text{H}(\text{Et}_2\text{O})_2]^+(\text{tftb})$ failed as the stability of bis(diethyloxonium) protonated intermediates strongly depends on the ligand species, and as a result, the reaction with insoluble CaH_2 reagents to form H_2 gas is too slow compared to the decomposition of the starting material.

The successful synthesis and purification of the two salts, $\text{Ca}[\text{Al}(\text{tftb})_4]_2$ and $\text{Ca}[\text{Al}(\text{hfip})_4]_2$, allow us to verify if the theoretical prediction that $[\text{Al}(\text{tftb})_4]^-$ will lead to a more reductively stable calcium salt and explore the other factors that influence the reductive stability (reflected as the Coulombic efficiency). To understand the electrochemical

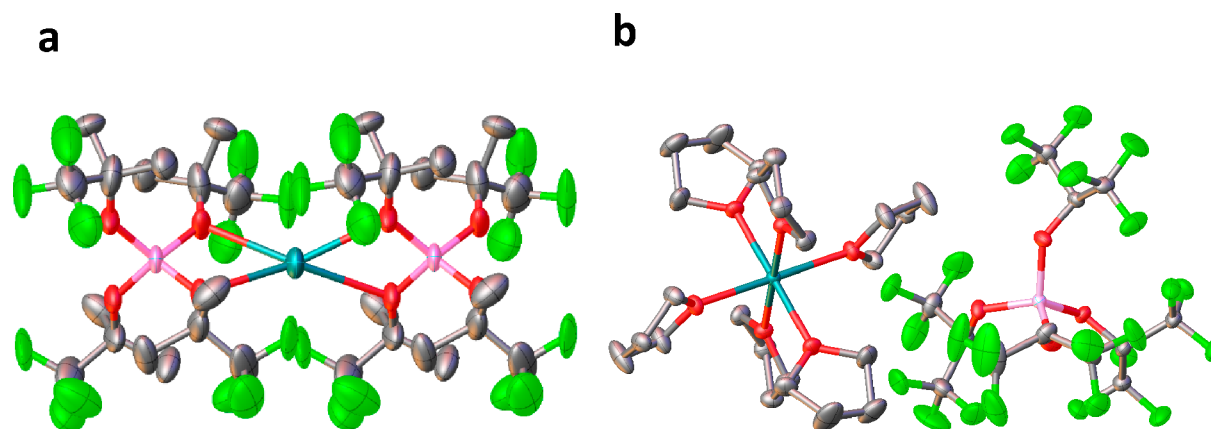


Figure 1. Single-crystal X-ray structures of (a) $\text{Ca}[\text{Al}(\text{tftb})_4]_2$ and (b) $\text{Ca}(\text{THF})_6[\text{Al}(\text{hfip})_4]_2$. Thermal ellipsoids are drawn at the 50% probability level. Hydrogen atoms are omitted for clarity. The other $[\text{Al}(\text{hfip})_4]^-$ anion is identical to the one shown and omitted for clarity. Green: fluorine, Gray: carbon, Blue: Calcium, Red: oxygen, Pink: Aluminum.

performance, it is imperative to identify both the purity and the structures of the new salts (as they are never reported experimentally) as they are crucial for the electrochemical performance. Initial insight into the structures of the two salts has been gained using single crystal X-ray diffraction.

The crystal structures of $\text{Ca}[\text{Al}(\text{tftb})_4]_2$ and $\text{Ca}[\text{Al}(\text{hfip})_4]_2$ are shown in Figure 1, unequivocally demonstrating that those compounds are pure. Despite the small change in ligands, the two calcium salt complexes exhibit significantly different solid state structures regarding coordination around Ca^{2+} : (1) contact ion paired (CIP) Ca^{2+} in the case of $\text{Ca}[\text{Al}(\text{tftb})_4]_2$ or (2) solvent-coordinated Ca^{2+} in a solvent-separated ion pair (SSIP) in the case of $\text{Ca}(\text{THF})_6[\text{Al}(\text{hfip})_4]_2$. Specifically, the presence of crystal-bound THF molecules is only observed in the case of $\text{Ca}(\text{THF})_6[\text{Al}(\text{hfip})_4]_2$, suggesting the more dissociative nature of $[\text{Al}(\text{hfip})_4]^-$, whereas $\text{Ca}[\text{Al}(\text{tftb})_4]_2$ prefers anion-coordinated Ca^{2+} . Transition-state calculations¹⁹ suggest that close contact ion pairing of magnesium trifluoromethanesulfonyl imide (MgTFSI_2) in diglyme electrolytes leads to a rapid decomposition of the TFSI anions upon reduction. As will be discussed later, electrochemical results confirm the solvent-coordinated Ca^{2+} formation in the solution of $\text{Ca}(\text{THF})_6[\text{Al}(\text{hfip})_4]_2$ is beneficial, with a high Coulombic efficiency, whereas the strongly ion paired Ca^{2+} in $\text{Ca}[\text{Al}(\text{tftb})_4]_2$ electrolytes is detrimental to performance. Note that solvation structures obtained in Figure 1 are solid-state single crystal solid structures, and more complex solvation structures can be present in solution. Similar magnesium electrolyte environments were observed before.²⁰ Therefore, further solvation studies were carried out in NMR, vibrational spectroscopy, and impedance studies.

Using NMR spectroscopy, we also demonstrate that $\text{Ca}(\text{THF})_6[\text{Al}(\text{hfip})_4]_2$ shows a preference for solvent-coordinated Ca^{2+} in SSIPs, whereas $\text{Ca}[\text{Al}(\text{tftb})_4]_2$ exhibits a tendency for strong cation–anion coordination, even in solution. Figure S6 illustrates this noteworthy finding of NMR characterization, revealing an unusual phenomenon wherein $\text{Ca}[\text{Al}(\text{tftb})_4]_2$ displays multiple methyl signals in proton NMR, and a comparable anomaly is observed for the CF_3 signal in fluorine NMR. This suggests the existence of a partially solvated CIP, similar to what is seen in the solid-state structure. The presence of two methyl and two trifluoromethyl signals in the NMR spectra indicates two distinct chemical environments for each group, without a dynamic exchange.

The introduction of an azacrown ether (K222), which is a chelating agent for Ca^{2+} and promotes separation of anion and cation coordination, proves instrumental in promoting the separation of ions and distinct peaks. Notably, these separated entities (-84.8 and -84.9 ppm) subsequently converge to a single peak (-85.1 ppm) in NMR spectra (Figure S6), underscoring the influence of this additive on the dynamic equilibrium within the solution. The $\text{Ca}[\text{Al}(\text{hfip})_4]_2$, on the other hand, has only one peak in the CF_3 region in the spectrum of its ^{19}F NMR, consistent with a single population of solvent coordinated Ca^{2+} and anions.

By comparing between the ionic conductivity measured through pulsed field gradient (pfg)-NMR self-diffusion and that obtained from electrochemical impedance spectroscopy, $\Lambda_{\text{imp}}/\Lambda_{\text{NMR}}$ ²¹ additional insights can be gained into the cation–anion association behavior. Both electrolytes exhibit large resistivity compared to their lithium counterparts; however, the difference between $\text{Ca}[\text{Al}(\text{tftb})_4]_2$ and $\text{Ca}[\text{Al}(\text{hfip})_4]_2$ is also pronounced. While the solution of $\text{Ca}[\text{Al}(\text{hfip})_4]_2$ has a moderate ionic conductivity (6×10^{-4} to 1.4×10^{-3} S/cm) with varying temperatures, the ionic conductivity of the solution of $\text{Ca}[\text{Al}(\text{tftb})_4]_2$ of the same concentration is negligible (Supporting Information Figure S13), further indicating that $\text{Ca}[\text{Al}(\text{tftb})_4]_2$ is less dissociative and predominantly forms coordination between Ca^{2+} and the $[\text{Al}(\text{tftb})_4]^-$ in the solution. Note that the solubility of both salts is not a problem as they both dissolve up to 0.4 M in DME. Furthermore, FTIR analysis conducted at different concentrations ranging from 0.1 to 0.4 M (Figure S9) reveals no change occurs in the IR stretching band of between $1350\text{--}1150$ cm^{-1} and $1000\text{--}900$ cm^{-1} , which are the features of mixed C–C and C–F stretches. This suggests that the coordination does not change significantly in this concentration and likely indicates that anion-coordinated Ca^{2+} is favored in solutions of $\text{Ca}[\text{Al}(\text{tftb})_4]_2$, regardless of concentration. The solution of $\text{Ca}[\text{Al}(\text{hfip})_4]_2$ on the other hand shows a distinct red shift with increased concentration, indicating Ca^{2+} coordinates less with $[\text{Al}(\text{hfip})_4]^-$ at lower concentrations (Figure S9).

The interactions between the cation, solvent, and anions, as well as the solvation structure, can also be experimentally viewed through an ionization mass spectrometry method.²² In order to understand the cation solvation environment, as well as the role of anion, we carried out Electrospray Ionization

Mass Spectrometry (ESI-MS) using both negative and positive ion mode. ESI-MS is a method capable of detecting solvation structures in solution, although slightly different solvation structures can be observed with different ESI-MS conditions, particularly cone and extractor voltages.²³ As shown in Figure 2, the results agree with the strong Ca^{2+} coordination in

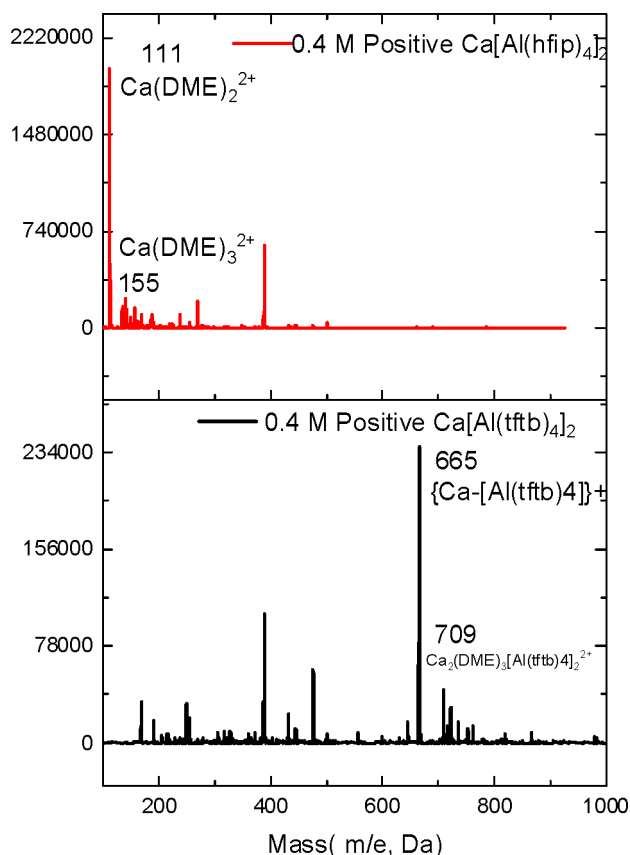


Figure 2. Typical mass spectra via electrospray ionization of $\text{Ca}[\text{Al}(\text{tftb})_4]_2$ and $\text{Ca}[\text{Al}(\text{hfip})_4]_2$ showing the different solvation environment between them.

$\text{Ca}[\text{Al}(\text{tftb})_4]_2$, as $\{\text{Ca}-[\text{Al}(\text{tftb})_4]\}^+$ species are detected in both high (0.4 M) and low concentration (0.1 M) electrolytes.

In contrast, $\text{Ca}[\text{Al}(\text{hfip})_4]_2$ predominantly exhibits $\text{Ca}(\text{DME})_2^{2+}$ and $\text{Ca}(\text{DME})_3^{2+}$ and the $[\text{Al}(\text{hfip})_4]^-$, consistent with the solvent-coordinated Ca^{2+} and anions indicated above. Due to the intricate nature of the ESI-MS spectra, our efforts to discern all peaks in Figure 2 were met with challenges. Consequently, we primarily relied on the detection of solvated Ca^{2+} as the primary indicator for the presence of solvent-coordinated Ca^{2+} .

To better contextualize the new insights provided by our experimental results, we utilized first-principles calculations to compare the formation free energies and specific solvation structures of Ca electrolytes under implicit DME solvent conditions. The specifics of the formation free energies are detailed in Section 4 of the Supporting Information (eqs S1 and S2). The results are displayed in Figure S16 as a heat map, illustrating the propensity for the formation of various solvated structures with different degrees of solvation. Notably, the solvation structure of $[\text{Al}(\text{hfip})_4]^-$ shows a preference for solvent-coordinated Ca^{2+} . In contrast $[\text{Al}(\text{tftb})_4]^-$ tends to favor the strong cation–anion coordination of $\text{Ca}[\text{Al}(\text{tftb})_4]_2$, similar to what we have observed experimentally.

The difference in the cation–anion association between $\text{Ca}[\text{Al}(\text{tftb})_4]_2$ and $\text{Ca}[\text{Al}(\text{hfip})_4]_2$ is further manifested in their electrochemical plating and stripping behavior. Note that all stripping and plating was conducted at ambient temperatures with a nonalloying glassy carbon electrode.²⁴ As shown in Figure 3, the difference between $\text{Ca}[\text{Al}(\text{tftb})_4]_2$ and $\text{Ca}[\text{Al}(\text{hfip})_4]_2$ is dramatic, with 0.1 M $\text{Ca}[\text{Al}(\text{hfip})_4]_2$ in DME exhibiting a Coulombic efficiency (CE) of 57%, whereas 0.1 M $\text{Ca}[\text{Al}(\text{tftb})_4]_2$ results in only Ca metal plating and no discernible stripping (0% CE).

These electrochemical data corroborate our observations of Ca^{2+} coordination above, and help to explain the partially reversible activity of $\text{Ca}[\text{Al}(\text{hfip})_4]_2$, in comparison to $\text{Ca}[\text{Al}(\text{tftb})_4]_2$. In particular, the improved electrochemical stability and reversibility correlate with the formation of solvent-coordinated Ca^{2+} , suggesting that the cation–anion ion pair structures formed in $\text{Ca}[\text{Al}(\text{tftb})_4]_2$ are too strong to enable reversible electrochemistry. It is also possible that $[\text{Al}(\text{tftb})_4]^-$ passivates Ca metal. Indeed, there are mixed reports on the role of the anion in guiding reversible Ca metal plating and stripping. Some view cation–anion association as

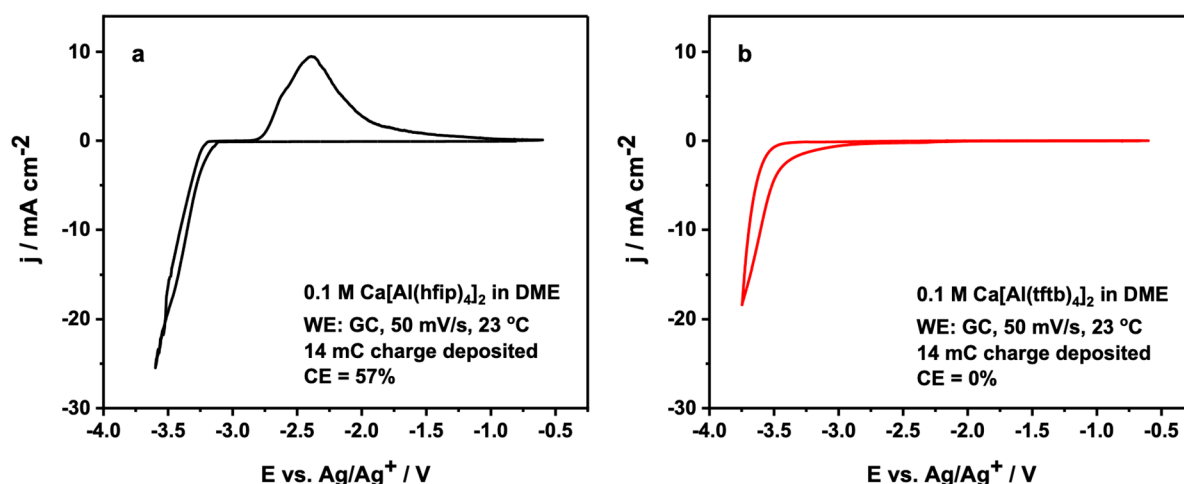


Figure 3. Cyclic voltammetry of 0.1 M $\text{Ca}[\text{Al}(\text{hfip})_4]_2$ and $\text{Ca}[\text{Al}(\text{tftb})_4]_2$ solution in DME. The sweep rate is 50 mV s^{-1} , and a fixed charge of 14 mC was passed on deposition for all CVs.; the exact condition can be found in the Supporting Information.

harmful, as it promotes further charge transfer decay¹⁹ as well as detrimental effects on transport, with slower migration across the SEI,⁴ while other reports suggest that cation–anion association can facilitate the formation of an anion-derived interphase film that enable reversible Ca plating and stripping better than solvent-derived films.²⁵ Our recent work in multianion electrolytes suggests that the relative strength of anion–cation association, rather than the presence or absence of contact ion pairs, is ultimately what controls electrolyte performance.²⁶ Our work here clearly demonstrates that anions that are too strongly coordinating lead to poor performance and the necessity to balance the anion–cation association strength to get electrolytes with optimal performance. It is clear that strongly coordinating cation anion interactions are more detrimental for Coulombic efficiency, as in the case of Ca[Al(tftb)₄]₂, while reversible activity is observed for the solvent-coordinated Ca²⁺ and SSIPs in the case of Ca[Al(hfip)₄].

Using a one-pot strategy, we have developed an innovative route to synthesize several calcium alkoxyaluminate salts for the first time. Two of these salts, Ca[Al(hfip)₄]₂ and Ca[Al(tftb)₄]₂, are of particular interest as they exhibit significantly different coordination structures in solution. Using a combination of spectroscopic and electrochemical analysis, we unambiguously identify the solvation and electrochemical performance difference in these two salts, which shows that these electrolytes are not universally weakly coordinating and that the strongly associated salt performs significantly worse than the one with weaker association. With that information we can envision further research aided design in which we can consider structures that optimize the strength of Ca²⁺ coordination to enable improved reductive stability and overall reversibility.

■ ASSOCIATED CONTENT

SI Supporting Information

The Supporting Information is available free of charge at <https://pubs.acs.org/doi/10.1021/acs.jpcllett.4c00969>.

Additional experimental details, materials, and methods, including NMR and other spectra. (PDF)

Transparent Peer Review report available (PDF)

■ AUTHOR INFORMATION

Corresponding Author

Chen Liao – *Chemical Sciences and Engineering Division, Argonne National Laboratory, Lemont, Illinois 60439, United States; Joint Center for Energy Storage Research, Lemont, Illinois 60439, United States; orcid.org/0000-0001-5168-6493; Email: liao@anl.gov*

Authors

Noel J. Leon – *Chemical Sciences and Engineering Division, Argonne National Laboratory, Lemont, Illinois 60439, United States; Joint Center for Energy Storage Research, Lemont, Illinois 60439, United States*

Stefan Ilic – *Joint Center for Energy Storage Research, Lemont, Illinois 60439, United States; Materials Science Division, Argonne National Laboratory, Lemont, Illinois 60439, United States; orcid.org/0000-0002-6305-4001*

Xiaowei Xie – *Joint Center for Energy Storage Research, Lemont, Illinois 60439, United States; Molecular Foundry Lawrence Berkeley National Laboratory, Berkeley, California*

94720, United States; Department of Materials Science and Engineering, University of California, Berkeley, California 94720, United States; orcid.org/0000-0001-5618-8768

Heonjae Jeong – *Joint Center for Energy Storage Research, Lemont, Illinois 60439, United States; Materials Science Division, Argonne National Laboratory, Lemont, Illinois 60439, United States; orcid.org/0000-0003-4452-049X*

Zhenzhen Yang – *Chemical Sciences and Engineering Division, Argonne National Laboratory, Lemont, Illinois 60439, United States; Joint Center for Energy Storage Research, Lemont, Illinois 60439, United States; orcid.org/0000-0002-1073-3799*

Bingning Wang – *Chemical Sciences and Engineering Division, Argonne National Laboratory, Lemont, Illinois 60439, United States; Joint Center for Energy Storage Research, Lemont, Illinois 60439, United States*

Evan Walter Clark Spotte-Smith – *Joint Center for Energy Storage Research, Lemont, Illinois 60439, United States; Molecular Foundry Lawrence Berkeley National Laboratory, Berkeley, California 94720, United States; Department of Materials Science and Engineering, University of California, Berkeley, California 94720, United States; orcid.org/0000-0003-1554-197X*

Charlotte Stern – *Department of Chemistry, Northwestern University, Evanston, Illinois 60208, United States; orcid.org/0000-0002-9491-289X*

Nathan Hahn – *Joint Center for Energy Storage Research, Lemont, Illinois 60439, United States; Material, Physical, and Chemical Sciences Center, Sandia National Laboratories, Albuquerque, New Mexico 87185, United States; orcid.org/0000-0001-6187-4068*

Kevin Zavadil – *Joint Center for Energy Storage Research, Lemont, Illinois 60439, United States; Material, Physical, and Chemical Sciences Center, Sandia National Laboratories, Albuquerque, New Mexico 87185, United States; orcid.org/0000-0002-3791-424X*

Lei Cheng – *Joint Center for Energy Storage Research, Lemont, Illinois 60439, United States; Materials Science Division, Argonne National Laboratory, Lemont, Illinois 60439, United States; orcid.org/0000-0002-3902-1680*

Kristin A. Persson – *Joint Center for Energy Storage Research, Lemont, Illinois 60439, United States; Molecular Foundry Lawrence Berkeley National Laboratory, Berkeley, California 94720, United States; Department of Materials Science and Engineering, University of California, Berkeley, California 94720, United States*

Justin G. Connell – *Joint Center for Energy Storage Research, Lemont, Illinois 60439, United States; Materials Science Division, Argonne National Laboratory, Lemont, Illinois 60439, United States; orcid.org/0000-0002-2979-2131*

Complete contact information is available at:

<https://pubs.acs.org/doi/10.1021/acs.jpcllett.4c00969>

Notes

The authors declare no competing financial interest.

■ ACKNOWLEDGMENTS

This work was led and supported by the Joint Center for Energy Storage Research (JCESR), an Energy Innovation Hub funded by the U.S. Department of Energy. Sandia National Laboratories is a multimission laboratory managed and operated by National Technology & Engineering Solutions

of Sandia, LLC, a wholly owned subsidiary of Honeywell International Inc., for the U.S. Department of Energy's National Nuclear Security Administration under contract DE-NA0003525. This paper describes objective technical results and analysis. Any subjective views or opinions that might be expressed in the paper do not necessarily represent the views of the U.S. Department of Energy or the United States Government. This research used resources of the Argonne National Laboratory, supported by the U.S. Department of Energy under contract no. DE-AC02-06CH11357. This work made use of the IMSERC Crystallography facility at Northwestern University, which has received support from the Soft and Hybrid Nanotechnology Experimental (SHyNE) Resource (NSF ECCS-2025633), and Northwestern University. We gratefully acknowledge the use of the Bebop or Swing or Blues cluster in the Laboratory Computing Resource Center at Argonne National Laboratory.

REFERENCES

- (1) Leon, N. J.; He, M.; Liao, C. Solvation, Rational Design, and Interfaces: Development of Divalent Electrolytes. *Front. Energy Res.* **2022**, *9*, Mini Review. DOI: 10.3389/fenrg.2021.802398.
- (2) Trahey, L.; Brushett, F. R.; Balsara, N. P.; Ceder, G.; Cheng, L.; Chiang, Y.-M.; Hahn, N. T.; Ingram, B. J.; Minteer, S. D.; Moore, J. S.; et al. Energy storage emerging: A perspective from the Joint Center for Energy Storage Research. *Proc. Nat. Acad. Sci.* **2020**, *117* (23), 12550–12557.
- (3) Kwon, B. J.; Yin, L.; Park, H.; Parajuli, P.; Kumar, K.; Kim, S.; Yang, M.; Murphy, M.; Zapol, P.; Liao, C.; et al. High Voltage Mg-Ion Battery Cathode via a Solid Solution Cr–Mn Spinel Oxide. *Chem. Mater.* **2020**, *32* (15), 6577–6587 (accessed 2021-01-26T04:12:54).
- (4) Wang, D.; Gao, X.; Chen, Y.; Jin, L.; Kuss, C.; Bruce, P. G. Plating and stripping calcium in an organic electrolyte. *Nat. Mater.* **2018**, *17* (1), 16–20.
- (5) Shyamsunder, A.; Blanc, L. E.; Assoud, A.; Nazar, L. F. Reversible Calcium Plating and Stripping at Room Temperature Using a Borate Salt. *ACS Energy Lett.* **2019**, *4* (9), 2271–2276.
- (6) Li, Z.; Fuhr, O.; Fichtner, M.; Zhao-Karger, Z. Towards stable and efficient electrolytes for room-temperature rechargeable calcium batteries. *Energy Environ. Sci.* **2019**, *12*, 3496.
- (7) Leon, N. J.; Xie, X.; Yang, M.; Driscoll, D. M.; Connell, J. G.; Kim, S.; Seguin, T.; Vaughney, J. T.; Balasubramanian, M.; Persson, K. A.; Liao, C. Room-Temperature Calcium Plating and Stripping Using a Perfluoroalkoxyaluminate Anion Electrolyte. *J. Phys. Chem. C* **2022**, *126* (32), 13579–13584.
- (8) Kisu, K.; Kim, S.; Shinohara, T.; Zhao, K.; Züttel, A.; Orimo, S.-I. Monocarbonyl cluster as a stable fluorine-free calcium battery electrolyte. *Sci. Rep.* **2021**, *11* (1). DOI: 10.1038/s41598-021-86938-0.
- (9) Ren, W.; Wu, D.; NuLi, Y.; Zhang, D.; Yang, Y.; Wang, Y.; Yang, J.; Wang, J. An Efficient Bulky Mg[B(Otfe)₄]₂ Electrolyte and Its Derivatively General Design Strategy for Rechargeable Magnesium Batteries. *ACS Energy Lett.* **2021**, *6* (9), 3212–3220.
- (10) Schmidt, A.; Koger, H.; Barthélemy, A.; Studer, G.; Esser, B.; Krossing, I. Is One of the Least Coordinating Anions Suitable to Serve as Electrolyte Salt for Magnesium-Ion Batteries? *Batteries & Supercaps* **2022**, *5* (12), No. e202200340.
- (11) Zhao-Karger, Z.; Gil Bardaji, M. E.; Fuhr, O.; Fichtner, M. A new class of non-corrosive, highly efficient electrolytes for rechargeable magnesium batteries. *J. Mater. Chem. A* **2017**, *5* (22), 10815–10820 (accessed 2021-02-11T02:18:29).
- (12) Lau, K.-C.; Seguin, T. J.; Carino, E. V.; Hahn, N. T.; Connell, J. G.; Ingram, B. J.; Persson, K. A.; Zavadil, K. R.; Liao, C. Widening Electrochemical Window of Mg Salt by Weakly Coordinating Perfluoroalkoxyaluminate Anion for Mg Battery Electrolyte. *J. Electrochem. Soc.* **2019**, *166* (8), A1510–A1519.
- (13) Herb, J. T.; Nist-Lund, C. A.; Arnold, C. B. A Fluorinated Alkoxyaluminate Electrolyte for Magnesium-Ion Batteries. *ACS Energy Lett.* **2016**, *1* (6), 1227–1232.
- (14) Xie, X.; Leon, N. J.; Small, D. W.; Spotte-Smith, E. W. C.; Liao, C.; Persson, K. A. Reductive Decomposition Kinetics and Thermodynamics That Govern the Design of Fluorinated Alkoxyaluminate/Borate Salts for Mg-Ion and Ca-Ion Batteries. *J. Phys. Chem. C* **2022**, *126* (49), 20773–20785. Jeong, H.; Kamphaus, E. P.; Redfern, P. C.; Hahn, N. T.; Leon, N. J.; Liao, C.; Cheng, L. Computational Predictions of the Stability of Fluorinated Calcium Aluminate and Borate Salts. *ACS Appl. Mater. Interfaces* **2023**, *15* (5), 6933–6941.
- (15) Yang, M.; Driscoll, D. M.; Balasubramanian, M.; Liao, C. Solvation Structure and Electrochemical Properties of a New Weakly Coordinating Aluminate Salt as a Nonaqueous Electrolyte for Zinc Batteries. *J. Electrochem. Soc.* **2020**, *167* (16), No. 160529.
- (16) Pavčnik, T.; Forero-Saboya, J. D.; Ponrouch, A.; Robba, A.; Dominko, R.; Bitenc, J. A novel calcium fluorinated alkoxyaluminate salt as a next step towards Ca metal anode rechargeable batteries. *J. Mater. Chem. A* **2023**, *11* (27), 14738–14747.
- (17) Pavčnik, T.; Lozinšek, M.; Pirnat, K.; Vizintin, A.; Mandai, T.; Aurbach, D.; Dominko, R.; Bitenc, J. On the Practical Applications of the Magnesium Fluorinated Alkoxyaluminate Electrolyte in Mg Battery Cells. *ACS Appl. Mater. Interfaces* **2022**, *14* (23), 26766–26774.
- (18) Krossing, I.; Raabe, I. Noncoordinating Anions—Fact or Fiction? A Survey of Likely Candidates. *Angew. Chem., Int. Ed.* **2004**, *43* (16), 2066–2090.
- (19) Rajput, N. N.; Qu, X.; Sa, N.; Burrell, A. K.; Persson, K. A. The Coupling between Stability and Ion Pair Formation in Magnesium Electrolytes from First-Principles Quantum Mechanics and Classical Molecular Dynamics. *J. Am. Chem. Soc.* **2015**, *137* (9), 3411–3420.
- (20) Pan, B.; Huang, J.; Sa, N.; Brombosz, S. M.; Vaughney, J. T.; Zhang, L.; Burrell, A. K.; Zhang, Z.; Liao, C. MgCl₂: The Key Ingredient to Improve Chloride Containing Electrolytes for Rechargeable Magnesium-Ion Batteries. *J. Electrochem. Soc.* **2016**, *163* (8), A1672.
- (21) Tokuda, H.; Tsuzuki, S.; Susan, M. A. B. H.; Hayamizu, K.; Watanabe, M. How Ionic Are Room-Temperature Ionic Liquids? An Indicator of the Physicochemical Properties. *J. Phys. Chem. B* **2006**, *110* (39), 19593–19600. Xu, K. Navigating the minefield of battery literature. *Commun. Mater.* **2022**, *3* (1), 31.
- (22) von Wald Cresce, A.; Gobet, M.; Borodin, O.; Peng, J.; Russell, S. M.; Wikner, E.; Fu, A.; Hu, L.; Lee, H.-S.; Zhang, Z.; et al. Anion Solvation in Carbonate-Based Electrolytes. *J. Phys. Chem. C* **2015**, *119* (49), 27255–27264. Son, S.-B.; Zhang, Z.; Gim, J.; Johnson, C. S.; Tsai, Y.; Kalensky, M.; Lopykinski, S.; Kahvecioglu, O.; Yang, Z.; Montoya, A. T.; Bloom, I. Transition Metal Dissolution in Lithium-Ion Cells: A Piece of the Puzzle. *J. Phys. Chem. C* **2023**, *127* (4), 1767–1775.
- (23) Zheng, D.; Qu, D.; Yang, X.-Q.; Lee, H.-S.; Qu, D. Preferential Solvation of Lithium Cations and Impacts on Oxygen Reduction in Lithium–Air Batteries. *ACS Appl. Mater. Interfaces* **2015**, *7* (36), 19923–19929. Fukushima, T.; Matsuda, Y.; Hashimoto, H.; Arakawa, R. Solvation of lithium ions in organic electrolytes of primary lithium batteries by electrospray ionization-mass spectroscopy. *J. Power Sources* **2002**, *110* (1), 34–37.
- (24) Ponrouch, A.; Frontera, C.; Bardé, F.; Palacín, M. R. Towards a calcium-based rechargeable battery. *Nat. Mater.* **2016**, *15* (2), 169–172.
- (25) Li, S.; Zhang, J.; Zhang, S.; Liu, Q.; Cheng, H.; Fan, L.; Zhang, W.; Wang, X.; Wu, Q.; Lu, Y. Cation replacement method enables high-performance electrolytes for multivalent metal batteries. *Nat. Energy* **2024**, *9*, 285.
- (26) Connell, J. G.; Zorko, M.; Agarwal, G.; Yang, M.; Liao, C.; Assary, R. S.; Strmcnik, D.; Markovic, N. M. Anion Association Strength as a Unifying Descriptor for the Reversibility of Divalent Metal Deposition in Nonaqueous Electrolytes. *ACS Appl. Mater. Interfaces* **2020**, *12* (32), 36137–36147. Driscoll, D. M.; Lavan, S. N.;

Zorko, M.; Redfern, P. C.; Ilic, S.; Agarwal, G.; Fister, T. T.; Assary, R. S.; Cheng, L.; Strmcnik, D.; et al. Emergent solvation phenomena in non-aqueous electrolytes with multiple anions. *Chem.* **2023**, *9* (7), 1955–1971. Ilic, S.; Lavan, S. N.; Leon, N. J.; Liu, H.; Jain, A.; Key, B.; Assary, R. S.; Liao, C.; Connell, J. G. Mixed-Anion Contact Ion-Pair Formation Enabling Improved Performance of Halide-Free Mg-Ion Electrolytes. *ACS Appl. Mater. Interfaces* **2024**, *16* (1), 435–443.